



# Finite Element Analysis of the Non-Equal Channel Angular Pressing (NECAP) with Different Die Geometries

A. Fardi-Ilkhchy, M. Shaban Ghazani\*

Department of Materials Science Engineering, University of Bonab, P.O.Box 5551761167, Bonab, Iran.

**ABSTRACT:** Non Equal Channel Angular Pressing is one of the promising severe plastic deformation techniques which is used to produce ultra-fine grained and nanostructured materials. In the present investigation, the deformation behavior of the Al 1100 alloy during the non-equal channel angular pressing was studied using two dimensional finite element simulations. Results showed that when the ratio of the width of the output to the input channel is higher than 0.7, the corner gap is formed in the outer side of the intersecting area of the two channels, and the amount of plastic strain decreases in the lower part of the sample. In contrast, when the amount of this ratio is lower than 0.7, the Dead Metal Zone is formed in the outer region of the intersecting area and the amount of strain is increased in the lower side of the sample. It is also observed that the uniformity of the applied plastic strain is decreased with the formation of Dead Metal Zone. In addition, the amount of damage factor is increased with increasing the ratio of the width of the output to the input channel, and the region with higher amounts of damage factors is shifted from the lower side to the middle region of the deformed sample. Finally, the results of FEM simulation showed that the amount of pressing force is decreased by increasing the width of the output channel.

## Review History:

Received: Jun. 27, 2020

Revised: Sep. 19, 2021

Accepted: Oct. 03, 2021

Available Online: Mar. 10, 2022

## Keywords:

Non-Equal Channel Angular Pressing

finite element analysis

strain

damage factor

Al 1100 alloy

## 1- Introduction

During the last decades, different severe plastic deformation methods have been used for producing ultra-fine grained and nanostructured metals and alloys [1]. The processed materials show improved mechanical properties compared with coarse grained counterparts [2]. Since deformation by using these methods leads to a reduction in the average size of grains, the strength and fracture toughness of the material increases simultaneously [3]. Additionally, the ultra-fine grained metals show the super-plastic deformation behavior at lower temperatures and higher strain rates compared with coarse-grained primary metals [4]. The most important severe plastic deformation methods introduced by the researchers include high pressure torsion [5], accumulative roll bonding [6], equal channel angular pressing [7], cyclic extrusion and compression [8], constrained groove pressing [9], and twist extrusion [10]. In the recent years, many new methods have been proposed to apply severe plastic deformation on materials with different shapes of initial samples [11-13]. Among these methods, Equal Channel Angular Extrusion (ECAE) is the most effective and simplest method that can be used for various metals and alloys. In this method, a sample with a circular or square cross-section is passed through the channels intersected with a sharp angle. The input and output channels of the die are intersected with an angle which is usually considered to be 90 degrees. A severe shear strain is applied to the sample when passing through the intersection

area of the two channels. However, since the cross-section of the input and output channels are equal, the deformation process can be repeated and a severe plastic strain can be imposed on the sample. In the recent years, the finite element analysis has been widely used to study the plastic deformation behavior of materials during equal channel angular pressing. In these investigations, the effects of different parameters such as ECAP die channel angle ( $\Phi$ ), friction between the sample and die channel wall, the outer curvature angle of the intersecting area of the channels ( $\Psi$ ), and various material properties have been studied in details [14]. On the other hand, researchers have presented modified versions of this method to overcome the disadvantages. For instance, ECAP in parallel channels [15] and rotary ECAP [16] have been introduced to eliminate the need for removing and reinserting deformed samples in to the channel of the ECAP die. Non-Equal Channel Angular Pressing (NECAP) is the ECAP process version which was used to process ultra-fine grained materials [17]. The principles of Non-Equal Channel Angular Pressing have been stated by Hasani et al. [18]. In their study, the theoretical principles have been discussed to describe the plastic strain imposed on the sample. Additionally, the deformation texture developed during this process has been analyzed. The study of scientific literature shows that the deformation behavior of materials during Non-Equal Channel Angular Pressing has not been investigated. Therefore, in the present research, the two-dimensional finite element analysis was employed to analyze the deformation characteristics of the Al11000 alloy during Non-Equal Channel Angular Pressing. The novelty of this study compared with the work

\*Corresponding author's email: m\_shaban@ubonab.ac.ir



of Hasani et al. [18] is that in the present investigation, the processing parameters such as strain distribution in the sample, uniformity of plastic deformation, damage factor distribution and the pressing load required for execution of this process have been studied.

## 2- Theoretical Background

In the present study, the DEFORM 2D software was used for two dimensional finite element simulation of NECAP process. The mechanical response of the material to the external forces and the flow behavior of the material is defined by stress-strain curves. In these curves, the stress and strain are effective based on the Von-Mises theory. The relationships of Von-Mises stress and strain with stress and strain component can be written as below:

$$\bar{\sigma}_{VM} = \frac{1}{\sqrt{2}} \sqrt{(\sigma_x - \sigma_y)^2 + (\sigma_y - \sigma_z)^2 + (\sigma_z - \sigma_x)^2 + 6(\tau_{xy}^2 + \tau_{yz}^2 + \tau_{zx}^2)}$$

$$\bar{\varepsilon}_{VM} = \frac{\sqrt{2}}{3} \sqrt{(\varepsilon_x - \varepsilon_y)^2 + (\varepsilon_x - \varepsilon_z)^2 + (\varepsilon_y - \varepsilon_z)^2}$$

The damage factor evaluated by DEFORM 2D can be used to predict the occurrence of fracture during cold forming processes. The damage factor increases as material is deformed. Afterwards, fracture occurs when the damage factor has reached its critical value. The critical value of damage factor can be defined using physical experimentation. In DEFORM 2D software, the damage factor is defined by the following equation:

$$D_f = \int_0^{\bar{\varepsilon}} \frac{\sigma^*}{\bar{\sigma}} d\varepsilon$$

Where  $\sigma^*$  is the tensile maximum principal stress,  $\bar{\sigma}$  is the effective stress, and  $d\varepsilon$  is the effective strain increment. Xia et al. [19] expressed a substituting discrete expression which was also suitable for the FE codes:

$$D_f \cong \sum_0^{t_f} \frac{\sigma^* \times \dot{\varepsilon} \times \Delta t}{\bar{\sigma}}$$

Where  $\dot{\varepsilon}$  is the equivalent strain rate,  $\Delta t$  is the variable time increment used in the FEM analysis, and  $t_f$  is the simulation time.

In the NECAP process, if  $T_i$  is considered to be the input channel thickness and  $T_0$  is the output channel thickness, the theoretical value of shear strain ( $\gamma$ ) in non-frictional conditions can be expressed by the following equation [18, 20]:

$$\gamma = \frac{T_i}{T_0} + \frac{T_0}{T_i}$$

In addition, the equivalent Von-Mises strain in the NECAP is obtained by the following equation [18]:

$$\varepsilon_{VM} = \frac{\gamma}{\sqrt{3}}$$

The basic partial differential equations for plain strain finite element simulation including body and inertia forces are as below:

$$G \left( \frac{\partial^2 u}{\partial x^2} + \frac{\partial^2 u}{\partial y^2} \right) + \frac{1}{1-2\nu} G \frac{\partial}{\partial x} \left( \frac{\partial u}{\partial x} + \frac{\partial v}{\partial y} \right) + X = \rho \frac{\partial^2 u}{\partial t^2}$$

$$G \left( \frac{\partial^2 v}{\partial x^2} + \frac{\partial^2 v}{\partial y^2} \right) + \frac{1}{1-2\nu} G \frac{\partial}{\partial x} \left( \frac{\partial u}{\partial x} + \frac{\partial v}{\partial y} \right) + Y = \rho \frac{\partial^2 v}{\partial t^2}$$

Where X and Y are the body forces for unit volume in the x and y directions,  $\rho$  is the density of material,  $\nu$  is Poisson ratio, G is shear modulus, and u and v are x and y displacements.

## 3- Finite Element Analysis

In the present study, the two dimensional finite element simulation was employed to analyze the deformation behavior of the Al 1100 alloy during Non-Equal Channel Angular Pressing. For this reason, the commercial code DEFORM 2D software was used. As for samples with square cross section, the plane strain conditions are dominated and the analysis was carried out in a two-dimensional manner [21, 22]. The working sample was assumed to be in a rectangular shape with dimensions of 20×50 mm and meshed with 4000 square elements. The mechanical properties of the Al 1100 alloy were imported in DEFORM 2D software as a true stress-true strain curve represented in Fig. 1. Die and plunger were considered as rigid parts. In addition, the friction coefficient between sample and die channel wall was set to 0.1, and the punch speed was assumed to be 0.1 mm/s. These assumptions were made to assess only the effect of die channel geometry on the deformation characteristics of the Al 1100 alloy during Non-Equal Channel Angular Pressing. It should be noted that the effect of temperature rise during deformation is ignored in this investigation [23], and therefore the selection of low punch speed of 0.1 mm/min is considered to meet this condition. Regarding the selection of friction coefficient in this study ( $\mu=0.1$ ), it should be emphasized that this parameter has an important effect on the strain distribution and deformation homogeneity in sample, during equal channel angular pressing [24]. As the aim of this research is not the evaluation of the effect of friction, the constant friction coefficient was considered in all simulation and its value is set to be 0.1 based on the similar works in the literature. In Non-Equal Channel

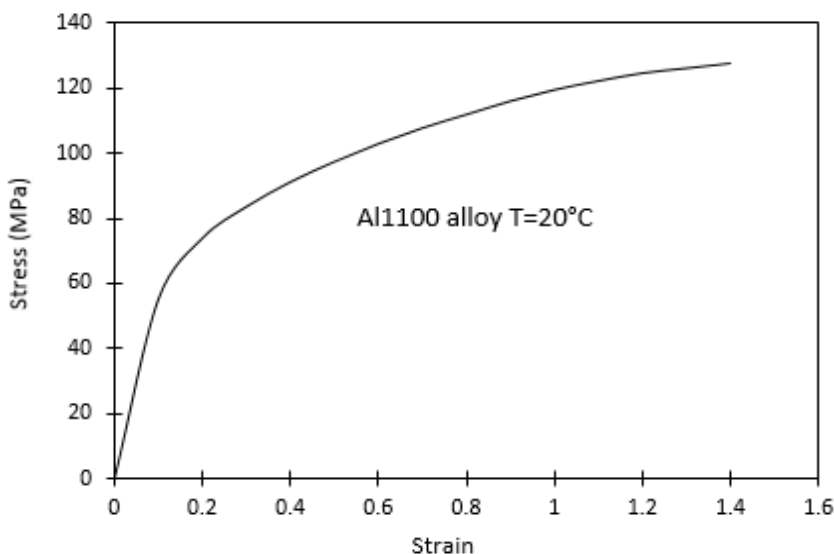


Fig. 1. Stress-strain curve of Al 1100 at room temperature.

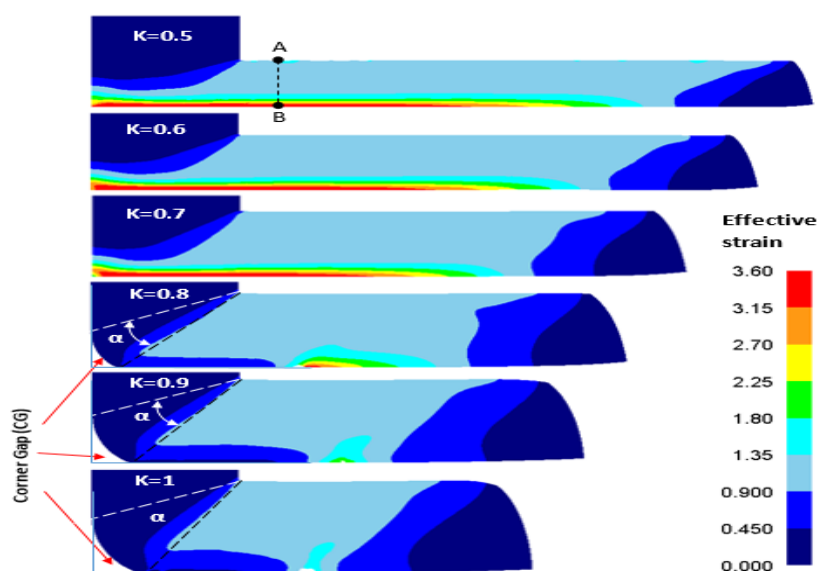


Fig. 2. Equivalent plastic strain distribution in sample during Non-equal channel angular pressing with different K coefficients.

Angular Pressing, the width of the output channel is lower than the width of input channel. Therefore, the ratio of the output channel to input channel width was demonstrated by K coefficient. The finite element analysis was carried out taking into account the different K values in the range of 0.5 to 1, and the effect of K parameter on different deformation characteristics was analyzed.

#### 4- Results and Discussion

##### 4- 1- Strain Distribution in the Sample

In Fig. 2, the distribution pattern of the effective strain in deformed specimen is shown after applying the plastic deformation using Non-Equal Channel Angular Pressing (NECAP). As demonstrated earlier, in this deformation

process the ratio of the output channel to the input channel width is demonstrated with K parameter. For instance, when the parameter K is considered to be 0.5, the output channel width is half the width of the input channel. It can be seen that for all values of K, the equivalent plastic strain is not uniformly distributed in the sample. By examining the distribution of the equivalent plastic strain in the samples, it is evident that for K in the range of 0.5 to 0.7, the maximum applied strain is related to the downside of the sample. In this case, the corner gap is not formed in the outer side of the intersecting area of two channels. However, for K values in the range of 0.8 to 1, the corner gap is evident in the intersecting area and the lower amounts of plastic strain are applied on the downside of the samples.

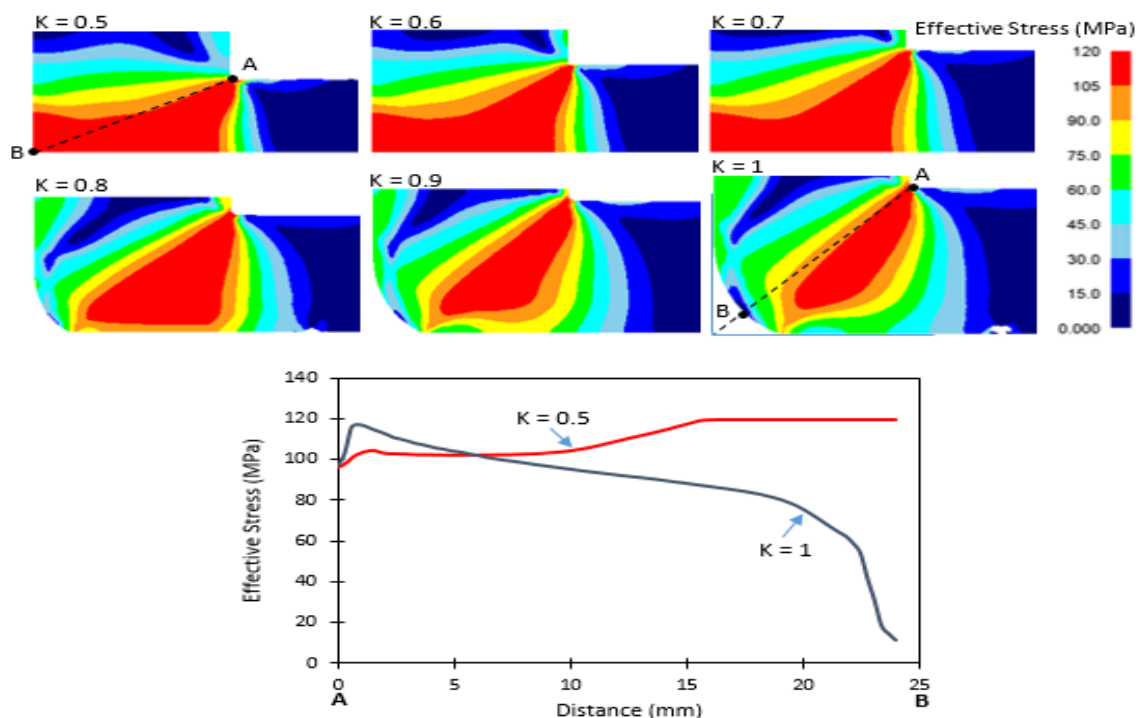


Fig. 3. Distribution of the effective stress in the deforming zone of the NECAP at different K values.

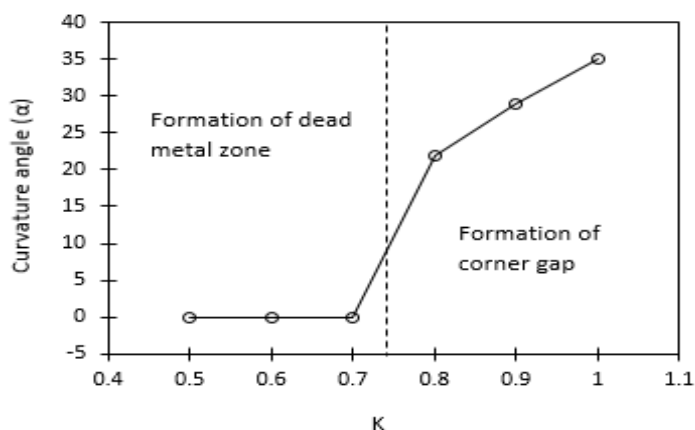


Fig. 4. Variations of the outer curvature angle of sample with K coefficient.

For further confirmation of these results, the variations of the effective stress during NECAP with different K values are shown in Fig. 3. As can be illustrated, for the samples NECAPed with the K factor of 0.5, 0.6, and 0.7, the maximum effective stress is related to the bottom side of the samples. However, for samples deformed with K factor of 0.8, 0.9, and 1 (in the case of the formation of the corner gap), the maximum effective stress is related to the topside of the sample. Additionally, there is a continuous decrease in the value of effective stress from point A to B. Having in mind the relation between effective stress and strain for materials ( $\sigma = k \varepsilon^n \dot{\varepsilon}^m$ , where  $\varepsilon$  is the effective strain,  $n$  is the strain hardening exponent,  $\dot{\varepsilon}$  is the strain rate,  $m$  is the strain rate

sensitivity, and  $k$  is a constant [25]), the higher effective stress applied on material results in the higher plastic strain. Therefore, for samples deformed in a die having the K factors of 0.5, 0.6, and 0.7, the higher amounts of plastic strain are observed on the bottom side of the sample. In contrast, for samples deformed in a die having the K factors of 0.8, 0.9, and 1, the lower amounts of plastic deformation is observed on the bottom side of the deformed samples. As can be seen in Fig. 2, the outer curvature angle of the samples is shown with the  $\alpha$  letter.

Fig. 4 shows the variation of the outer curvature angle of the sample ( $\alpha$ ) with the K coefficient. As can be demonstrated, for values of K in the range of 0.5 to 0.7, the outer curvature

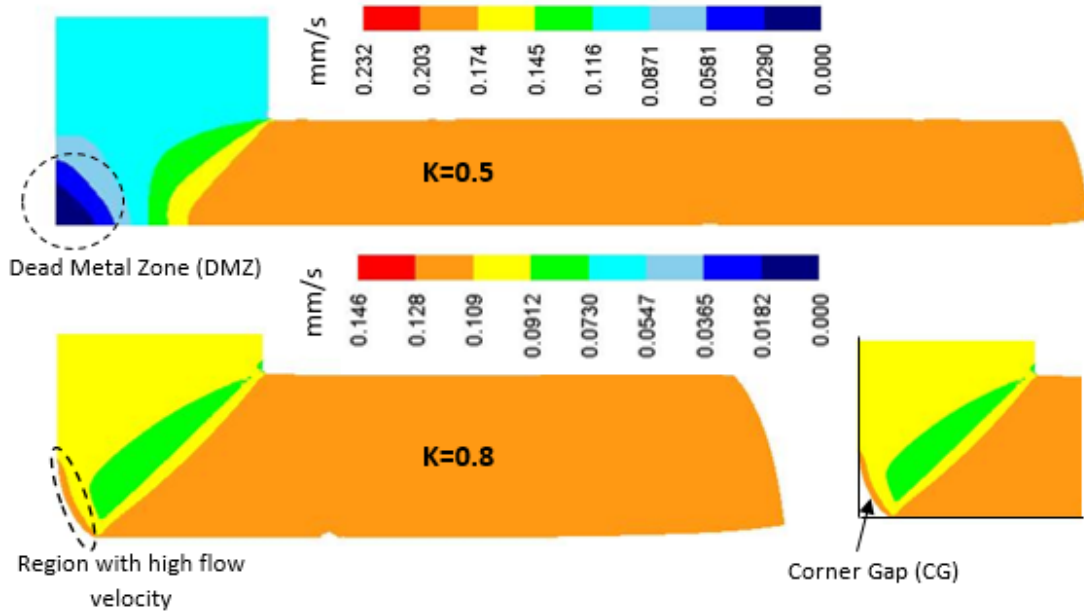


Fig. 5. Flow velocity distribution in sample during NECAP process with different values of K coefficient.

angle ( $\alpha$ ) is zero. It is also apparent that the outer curvature angle is non zero for K values higher than 0.7. It can be observed that the value of the  $\alpha$  angle is increased with K coefficient. Therefore, the formation of a corner gap has an influence on the strain distribution pattern of the deformed specimens. The lack of corner gap in the intersecting area of two channels leads to the formation of a highly deformed region in the lower side of sample and the formation of corner gap reduces the strain in these regions. The cause of the increase in strain applied to regions near the lower side of sample can be attributed to the formation of Dead Metal Zone in the outer side of the intersecting area.

In Fig. 5, the distribution of flow velocity in different regions of the sample is shown for K coefficients of 0.5 and 0.8. It can be seen that in the case of die with K coefficient equal to 0.5, the flow velocity of material is close to zero in the outer side of the intersecting area of two channels. This area is called the Dead Metal Zone (DMZ). With the formation of the Dead Metal Zone, and as a result of decrease in the flow velocity of material in this area, the amount of plastic strain is increased in the bottom side of the sample. It is important to note that the formation of dead zone in the outer region of the intersecting area results in higher amounts of shear deformation which imposes on a material moving against the material in the upper boundary of the Dead Metal Zone. This shear deformation is the reason for higher strains achieved in the bottom side of the sample. However, in the case of a K coefficient equal to 0.8, the flow velocity of the material in the outer side of the intersecting area of the channels is higher than the surrounding regions. Under such conditions, a corner gap is formed at the intersecting area, and the applied strain is decreased in the bottom side of the sample. Corner gap occurs during the ECAP of strain hardening materials, but perfect plastic materials deform uniformly through the cross section of the sample without the formation of a corner gap. For the strain hardening material, the inside part of the work-

piece within the deforming zone which receives more severe deformation, is harder than the outer part of the deforming zone. The outside part of the work-piece, which receives lower deformation and therefore is softer than the inside part within the deforming zone, can flow faster to the exit channel. The outside surface of the strain hardening work-piece goes through the shorter distance, and hence, the corner gap is formed and the bottom surface of the final work-piece of strain hardening material shows lower shear deformation than the non-hardening material [26].

In Fig. 6, the effective strain variations in the cross section of the deformed sample from the upper to lower side are represented for dies having different K coefficients. These curves can be divided in two different regions. Region I is related to the upper half of the deformed sample and shows no significant changes in the applied plastic strain. Region II shows significant variations in the amount of applied strain. It is demonstrated that in the case of dies with a K coefficient in the range of 0.5 to 0.7, the plastic strain is increased with moving toward the bottom side of the sample. Whereas, in the case of dies with K coefficient in the range of 0.8 to 1, the plastic strain is decreased with moving toward the bottom side of the deformed samples. These variations in the amounts of applied plastic strain result in the non-uniform microstructure.

In order to evaluate the strain uniformity, the coefficient of the variance of strain values in the cross section of the samples was calculated. The coefficient of the variance of plastic strain can be obtained by the following equation [27]:

$$CV_{\epsilon} = \frac{Stdev(\epsilon)}{Avg(\epsilon)} \quad (1)$$



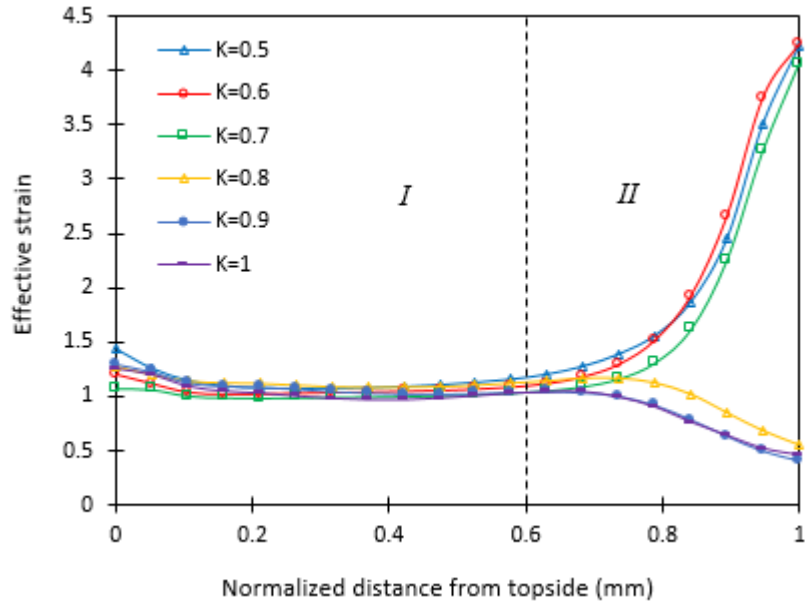


Fig. 6. Equivalent plastic strain variations across deformed sample during NECAP processing with different K coefficients.

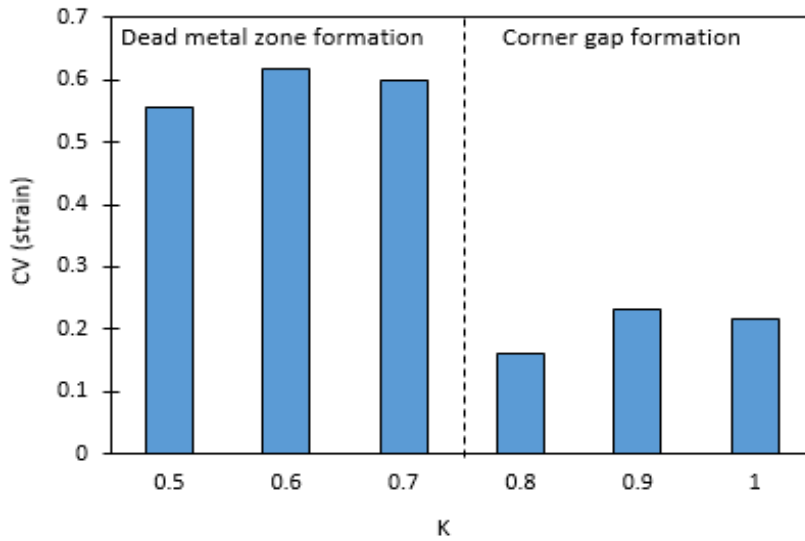


Fig. 7. Variations of the plastic strain inhomogeneity factor (CV) with K coefficient.

where  $Stdev(\epsilon)$  is the standard deviation of strain values, and  $Avg(\epsilon)$  is the average value of the strain in the cross section of deformed sample. According to this equation, the non-uniformity of applied plastic strain is increased with increasing the value of  $CV_{\epsilon}$ .

In Fig. 7, the variations of the coefficient of the variance of the strain values in the cross-section of deformed sample is shown as a function of the K coefficient. According to this diagram, it can be concluded that in high values of the K coefficient, which the corner gap is formed in the intersecting area of two channels, the uniformity of the applied strain is higher and by forming the Dead Metal Zone at low values of K, the strain distribution in the cross section of the deformed

sample becomes non-uniform. It is observed that the most non-uniform strain distribution is achieved when the K value is considered to be 0.6 and the most uniform plastic deformation is obtained when the K value equals to 0.9.

#### 4- 2- Damage Accumulation

In some cases, samples were cracked and fractured during processing with equal channel angular pressing. Under such conditions, applying more strain through the repetition of the deformation process is impossible. This case has been observed for brittle materials such as magnesium alloys with HCP crystalline structure [28]. In order to examine the possibility of the occurrence of fracture during severe plastic

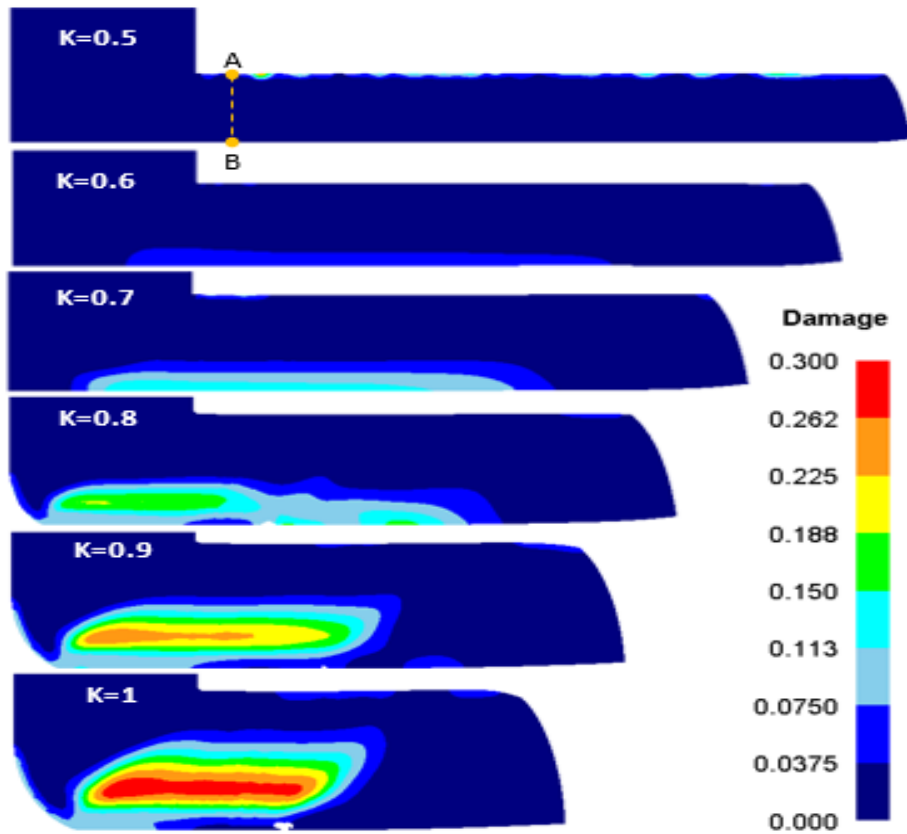


**Fig. 8. Damage distribution in sample during NECAP process with different values of K coefficient.**

deformation processes, the Kraft-Latham failure criterion is usually used. The value of the Kraft-Latham damage factor is calculated using the following equation [29]:

$$C = \int_0^{\epsilon_f} \frac{\sigma}{\bar{\sigma}} d\epsilon \quad (2)$$

where,  $\epsilon$  is the effective strain,  $\sigma$  is the maximum tensile stress, and  $\bar{\sigma}$  is equivalent stress. According to this equation, failure occurs through cracking when the amount of damage factor in the sample reaches a critical value. Therefore, when the distribution of the damage factor in the deformed sample is obtained, the region of the failure initiation can be determined. Therefore, regions with higher values of damage factor are prone to initiation of failure.

Fig. 8 represents the distribution of the Kraft-Latham damage factor in samples during Non-Equal Channel Angular Pressing with different K coefficients. In the case of NECAP dies with a K coefficient equal to 0.5, only a narrow region of the upper side of sample has a non-zero damage factor. Meanwhile, with increasing the K coefficient to 0.6, the damage factor is increased in the region located at the bottom side of the sample. In the case of the K coefficient equal to 0.7, the area with non-zero damage factor is enlarged.

Therefore, during Non-Equal Channel Angular Pressing with K coefficients lower than 0.8, when the Dead Metal Zone is formed the damage factor is non-zero at the region in the bottom side of sample and the extent of this region is increased with K coefficient. However, when K value is equal to 0.8 or higher and corresponding to the formation of the corner gap in the outer side of the intersecting area of channels, the higher levels of damage factor is obtained in the inner regions close to the bottom side of the sample. With increasing K coefficient from 0.8 to 1, the width of the region with non-zero damage factor is increased and this region is extended to the upper side of the sample. Fig. 9 (a) shows the variations of the damage factor in the cross section of sample during Non-Equal Channel Angular Pressing. Additionally, the variations of the maximum damage factor with K coefficient is illustrated in Fig. 9 (b). The trend of these variations is in such a manner that the maximum damage factor is achieved when K coefficient equals to 1 and the minimum damage is obtained when K coefficient is considered to be 0.6. Comparing the equivalent plastic strain distributions in Fig. 2 with damage distributions in Fig. 8, it is deduced that for K values of 0.5, 0.6, and 0.7, the damage factor and effective strain have a direct relation. It is obvious that when the damage is high at the bottom side of the sample, the effective strain is also higher than other regions. However, for K values of 0.8, 0.9 and 1, the damage and strain distributions have inverse relation. It is evident that

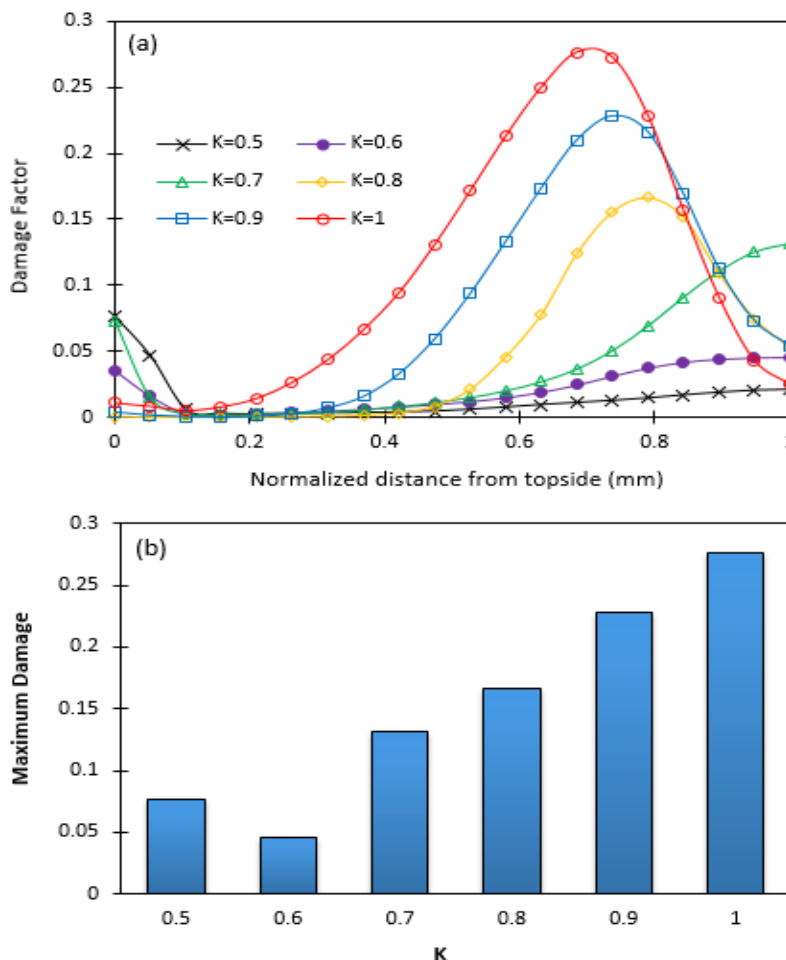


**Fig. 9. Variations of damage factor across deformed sample (a), and the variation of maximum damage with K coefficient during**

the strain in the bottom side of the sample is lower than the upper sides, but the damage values are higher at the bottom side of sample compared to the upper regions. It is worth to note that the damage factor is calculated using Eq. 2 and its magnitude is obtained by considering the cumulative effects of plastic strain, maximum tensile stress and equivalent stress. Therefore, the relation between applied strain and damage factor cannot be determined without considering the effects of other parameters.

#### 4- 3- Shape of Plastic Deformation Zone

In order to investigate the shape of the plastic deformation zone, the equivalent strain rate distribution in the sample is usually considered. Fig. 10 shows the distribution of strain rates in the samples in the intersecting area of the two channels. It should be noted that if the deformation during equal channel angular pressing is of a pure shear type, the plastic strain is applied on sample in the narrow region located in the intersecting area of the two channels. Therefore, any deviation from this state indicates the combination of shear and non-shear deformation. It is also worth to note that the shape of a region with non-zero strain rate represents the shape

of deformation zone. It is demonstrated that with increasing the amount of K coefficient, the deformation region becomes narrower and tends toward the intersecting plane of the two channels. Hence, it is concluded that in the lower values of K coefficient, the deformation zone is larger and the deviation from the pure shear deformation is greater. As K coefficient increases, the deformation zone becomes narrower and tends into a pure shear. However, in all K coefficients, the deformation is not of pure shear. Additionally, due to the work hardening of material as a result of the non-zero work hardening exponent, corner gap is formed in the intersecting area of two channels, which causes deviation from the pure shear deformation condition.

#### 4- 4- Pressing Force

Fig. 11 represents the variations of the pressing force during Non-Equal Channel Angular Pressing. As can be illustrated, the trends of the variations in the pressing force can be divided in to two different types. In the case of NECAP dies with K coefficients of 0.5, 0.6 and 0.7, the pressing force increases at the beginning of the process and finally reaches a constant and stable value. However, in the case of NECAP



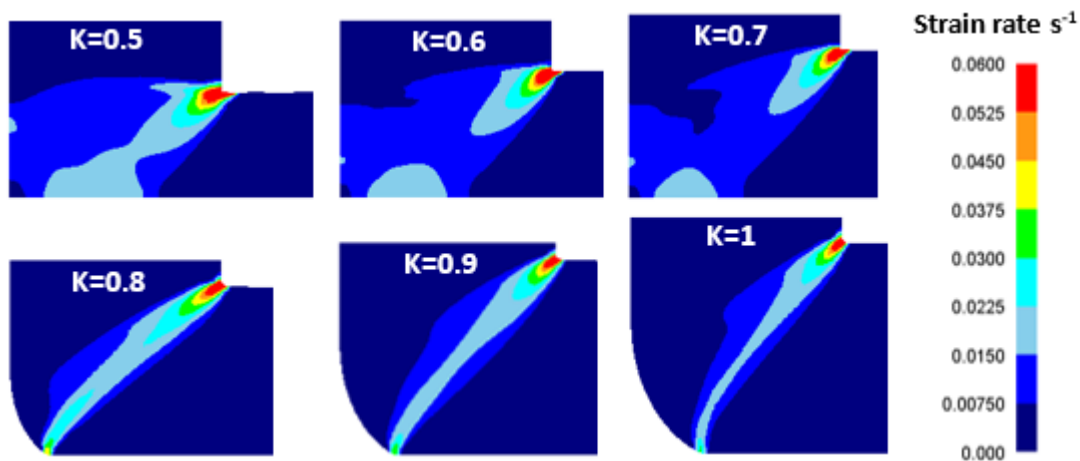


Fig. 10. The shape of deformation zone during NECAP with different K coefficients.

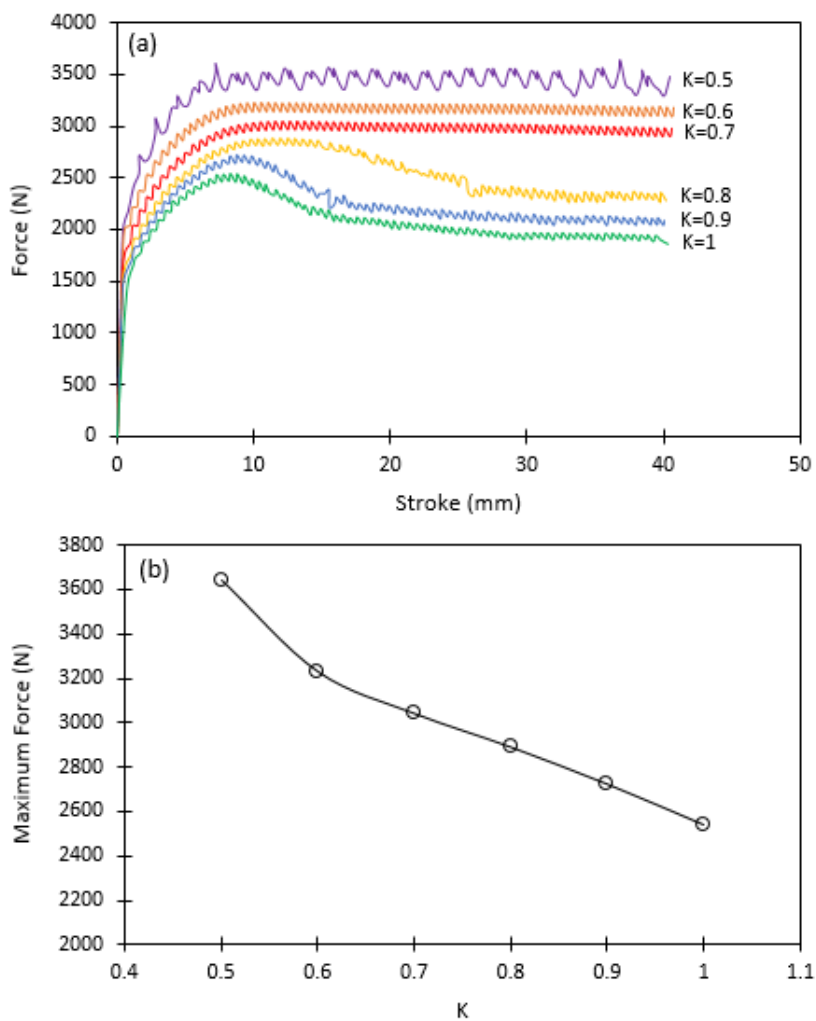


Fig. 11. Variations of pressing force during NECAP processing with different K coefficients (a), and the variations of maximum

dies with K coefficients of 0.8, 0.9 and 1, the pressing force increases with time at the beginning of the process and reaches a maximum value. Afterwards, the pressing force gradually decreases and later remains constant until the end of the deformation process. These two types of variations in the pressing force are related to the flow behavior of material during NECAP processing. When the Dead Metal Zone is formed at the intersecting area of two channels, the force-time curves represent the first trend. However, when the corner gap is formed at the intersecting area of the channels, the force-time curves indicate the second behavior. In addition, Fig. 9 (b) represents the variations of the maximum pressing force with K coefficient. It is demonstrated that the pressing force is increased with decreasing the value of K coefficient which corresponds to the decrease in the width of the output channel.

## 5- Conclusions

In the present study, deformation behavior of Al 1100 alloy during Non-Equal Channel Angular Pressing was investigated using two dimensional finite element analysis. The main results are as follows:

When the ratio of the width of the output channel to the width of the input channel (K coefficient) is equal to 0.5, 0.6 and 0.7, the Dead Metal Zone (DMZ) is formed in the outer side of the intersecting area of the two channels. The formation of this region is accompanied by an increase in the strain applied to the bottom side of the sample and greatly reduces the uniformity of the applied strain.

When the ratio of the width of the output channel to the input channel is 0.8, 0.9 and 1, the corner gap is formed in the outer side of the intersecting area of two channels and the amount of applied strain is decreased in the bottom side of the deformed sample.

By increasing K coefficient of the NECAP dies to 0.7, the outer curvature angle of the sample is zero. However, this parameter is increased gradually with further increase in K coefficient.

Considering K coefficients lower than 0.8, the maximum damage factor is attained in the region near the bottom side of deformed sample. With increasing the K coefficient, the width of the area with maximum damage is increased and this area is extended to the upper side of the sample.

The pressing force required for execution of NECAP process is increased with decreasing the width of the output channel.

## References

- [1] A. Azushima, R. Kopp, A. Korhonen, D. Yang, F. Micari, G. Lahoti, P. Groche, J. Yanagimoto, N. Tsuji, A. Rosochowski, Severe plastic deformation (SPD) processes for metals, *CIRP Annals*, 57(2) (2008) 716-735.
- [2] R. Valiev, N. Enikeev, M.Y. Murashkin, V. Kazykhanov, X. Sauvage, On the origin of the extremely high strength of ultrafine-grained Al alloys produced by severe plastic deformation, *Scripta Materialia*, 63(9) (2010) 949-952.
- [3] M. Calcagnotto, D. Ponge, D. Raabe, Effect of grain refinement to 1  $\mu\text{m}$  on strength and toughness of dual-phase steels, *Materials Science and Engineering: A*, 527(29-30) (2010) 7832-7840.
- [4] M. Kawasaki, N. Balasubramanian, T.G. Langdon, Flow mechanisms in ultrafine-grained metals with an emphasis on superplasticity, *Materials Science and Engineering: A*, 528(21) (2011) 6624-6629.
- [5] A.P. Zhilyaev, T.G. Langdon, Using high-pressure torsion for metal processing: Fundamentals and applications, *Progress in Materials Science*, 53(6) (2008) 893-979.
- [6] Y. Saito, H. Utsunomiya, N. Tsuji, T. Sakai, Novel ultra-high straining process for bulk materials—development of the accumulative roll-bonding (ARB) process, *Acta materialia*, 47(2) (1999) 579-583.
- [7] R.Z. Valiev, T.G. Langdon, Principles of equal-channel angular pressing as a processing tool for grain refinement, *Progress in materials science*, 51(7) (2006) 881-981.
- [8] J. Lin, Q. Wang, L. Peng, H.J. Roven, Microstructure and high tensile ductility of ZK60 magnesium alloy processed by cyclic extrusion and compression, *Journal of Alloys and Compounds*, 476(1-2) (2009) 441-445.
- [9] D.H. Shin, J.-J. Park, Y.-S. Kim, K.-T. Park, Constrained groove pressing and its application to grain refinement of aluminum, *Materials Science and Engineering: A*, 328(1-2) (2002) 98-103.
- [10] Y. Beygelzimer, D. Orlov, V. Varyukhin, A new severe plastic deformation method: twist extrusion, *Ultrafine grained materials II*, (2002) 297-304.
- [11] A. Babaei, M. Mashhadi, H. Jafarzadeh, Tube cyclic expansion-extrusion (TCEE) as a novel severe plastic deformation method for cylindrical tubes, *Journal of Materials Science*, 49(8) (2014) 3158-3165.
- [12] M. Ensafi, G. Faraji, H. Abdolvand, Cyclic extrusion compression angular pressing (CECAP) as a novel severe plastic deformation method for producing bulk ultrafine grained metals, *Materials Letters*, 197 (2017) 12-16.
- [13] S. Sepahi-Boroujeni, F. Fereshteh-Saniee, Expansion equal channel angular extrusion, as a novel severe plastic deformation technique, *Journal of materials science*, 50(11) (2015) 3908-3919.
- [14] F. Djavanroodi, M. Ebrahimi, Effect of die channel angle, friction and back pressure in the equal channel angular pressing using 3D finite element simulation, *Materials Science and Engineering: A*, 527(4-5) (2010) 1230-1235.
- [15] I. Sabirov, M. Perez-Prado, M. Murashkin, J. Molina-Aldareguia, E. Bobruk, N. Yunusova, R. Valiev, Application of equal channel angular pressing with parallel channels for grain refinement in aluminium alloys and its effect on deformation behavior, *International Journal of Material Forming*, 3(1) (2010) 411-414.
- [16] A. Ma, Y. Nishida, K. Suzuki, I. Shigematsu, N. Saito, Characteristics of plastic deformation by rotary-die equal-channel angular pressing, *Scripta Materialia*, 52(6) (2005) 433-437.
- [17] L.S. Tóth, R. Lapovok, A. Hasani, C. Gu, Non-Equal Channel Angular Pressing of aluminum alloy, *Scripta Materialia*, 61(12) (2009) 1121-1124.
- [18] A. Hasani, L.S. Toth, B. Beausir, Principles of nonequal channel angular pressing, *Journal of Engineering Materials and Technology*, 132 (2010) 031001.
- [19] Y. F Xia, G. Z Quan, Jie Zhou, Effects of temperature

- and strain rate on critical damage value of AZ80 magnesium alloy, *Transactions of Nonferrous Metals Society of China*, 20 (2010) s580-s583.
- [20] D. N Lee, An upper-bound solution of channel angular deformation, 43(2) (2000) 115-118.
- [21] A.V. Nagasekhar, H.S. Kim, Analysis of T-shaped equal channel angular pressing using the finite element method, *Metals and Materials International*, 14 (2008), 565-568.
- [22] A.V. Nagasekhar, H.S. Kim, Plastic deformation characteristics of cross-equal channel angular pressing, *Computational Materials Science*, 43(4) (2008) 1069-1073.
- [23] F. Djavanroodi, M. Ebrahimi, Effect of die channel angle, friction and back pressure in the equal channel angular pressing using 3D finite element simulation, *Materials Science and Engineering A*, 527(4-5) (2010) 1230-1235.
- [24] I. Balasundar, T. Raghu, Effect of friction model in numerical analysis of equal channel angular pressing process, *Materials and Design*, 31(1) (2010) 449-457.
- [25] D. Li, A. Ghosh, Tensile deformation behavior of aluminum alloys at warm forming temperatures, *Materials Science and Engineering: A*, 352(1-2) (2003) 279-286.
- [26] H.S. Kim, M.H. Seo, S.I. Hong, On the die corner gap formation in equal channel angular pressing, *Materials Science and Engineering: A*, 291(1-2) (2000) 86-90.
- [27] V.P. Basavaraj, U. Chakkingal, T.P. Kumar, Study of channel angle influence on material flow and strain inhomogeneity in equal channel angular pressing using 3D finite element simulation, *Journal of materials processing technology*, 209(1) (2009) 89-95.
- [28] R.B. Figueiredo, P.R. Cetlin, T.G. Langdon, The processing of difficult-to-work alloys by ECAP with an emphasis on magnesium alloys, *Acta Materialia*, 55(14) (2007) 4769-4779.
- [29] R.B. Figueiredo, P.R. Cetlin, T.G. Langdon, The evolution of damage in perfect-plastic and strain hardening materials processed by equal-channel angular pressing, *Materials Science and Engineering: A*, 518(1-2) (2009) 124-131.

#### HOW TO CITE THIS ARTICLE

A. Fardi-Ilkhchy and M. Shaban Ghazani, *Finite Element Analysis of the Non-Equal Channel Angular Pressing (NECAP) with Different Die Geometries*, *AUT J. Model. Simul.*, 53(2) (2021) 81-92.

DOI: [10.22060/miscj.2021.18646.5219](https://doi.org/10.22060/miscj.2021.18646.5219)



